ELSEVIER

Tectonophysics 329 (2000) 1–21

TECTONOPHYSICS

www.elsevier.com/locate/tecto

Evidence for crustal extension and inversion in eastern Tasmania, Australia, during the Neoproterozoic and Early Palaeozoic

B.J. Drummond[a,*], T.J. Barton[a,b], R.J. Korsch[a], N. Rawlinson[b], A.N. Yeates[a], C.D.N. Collins[a], A.V. Brown[c]

[a]*Australian Geological Survey Organisation, GPO Box 378, Canberra, Australian Capital Territory 2601, Australia*
[b]*Australian Geodynamics Cooperative Research Centre, Monash University, Clayton, Victoria 3168, Australia*
[c]*Mineral Resources Tasmania, PO Box 56, Rosny Park, Tasmania 7018, Australia*

Received 30 March 1999; accepted 3 January 2000

Abstract

The island of Tasmania in southeast Australia consists of a number of stratotectonic elements. The relationships between these elements are largely obscured by younger cover of the Tasmania Basin, which contains extensive dolerite sills that limit the ability of potential field techniques to map basement. Therefore the development of a robust tectonic model for Tasmania has been inhibited. To assist in the development of a tectonic model, a deep seismic reflection program undertaken offshore around the entire island was designed to map the large-scale structures of Tasmania at depth. The airgun seismic energy was also recorded at a number of seismographs deployed across the island, allowing low resolution 3D tomographic imaging. Short reflection profiles were recorded onshore across structures which could not be imaged by the offshore profiling. This paper focuses on eastern Tasmania. In the seismic sections, the Proterozoic basement in the southeast is mostly featureless, except for large rotated blocks with weakly reflective boundary faults, indicating extension of the Tyennan Element by block faulting. The deposition of the sedimentary succession of the Adamsfield–Jubilee Element was related to this extensional event. In the northeast, a reflective lower crust is interpreted to represent thrust slices of previously highly extended continental crust and possibly fragments of oceanic crust. The Early Palaeozoic sedimentary succession of the Northeast Tasmania Element formed across the inverted margin. The apparently complex geology of eastern Tasmania therefore fits into an extensional model where continental extension eventually led to the formation of very thin continental crust and possibly oceanic crust to the east. The extension was probably related to Late Neoproterozoic extension recorded elsewhere in Australia. The region was subsequently shortened, probably in a northeast–southwest direction, with most shortening accommodated in the seismically reflective, probably oceanic part of the crust, and little or no shortening in the block-faulted, and extended continental crust.

Keywords: crustal extension; inversion; Tasmania; Australia; Neoproterozoic

1. Introduction

Tasmania is an island state in southeast Australia. To place its known mineral and energy resources into a regional tectonic framework, a program of deep seismic reflection profiling and two- (2D) and

* Corresponding author. Tel.: +61-262-499381; fax: +61-262-499972.
E-mail address: barry.drummond@agso.gov.au (B.J. Drummond).

0040-1951/00/$ - see front matter
PII: S0040-1951(00)00185-2

three-dimensional (3D) seismic tomography was undertaken in 1995 by the Australian Geological Survey Organisation, working with Mineral Resources Tasmania under the Australian National Geoscience Mapping Accord. These data complement the comprehensive geological mapping, regional gravity and magnetic data sets that are available.

Geologically, Tasmania can be divided into a number of stratotectonic elements (Fig. 1a), each with a distinctly different chronostratigraphy and probably tectonic history (Seymour and Calver, 1995). Proterozoic rocks crop out in the Rocky Cape Element in the northwest and the Tyennan Element in the southwest. Late Proterozoic and Early to Middle Palaeozoic sedimentary and volcanic rocks of the Dundas Element lie between these two elements. Using seismic reflection data Drummond et al. (1996) showed that rocks of the Dundas Element extend to depths of 4–6 km, and cover a boundary between the Rocky Cape Element and the Tyennan Element that dips east at about 30° and probably extends through the crust.

Three other basement elements are defined east of the Tyennan Element. The Adamsfield–Jubilee contains Neoproterozoic to Early Devonian sedimentary rocks and onlaps the eastern side of Tyennan Element. The Northeast Tasmania Element contains folded Ordovician to Devonian sedimentary, mostly turbiditic, rocks of the Mathinna Group, which are intruded by extensive Devonian granitic rocks. Extensive granitoids intruded most elements from mid-Devonian to earliest Carboniferous times. The Sheffield Element in the central north (Fig. 1) is beyond the scope of this paper.

Sedimentary rocks and extensive dolerite sills of the post-Devonian Tasmania Basin obscure the relationship between the Tyennan and Adamsfield–Jubilee Elements in the west and the Northeast Tasmania Element. Although the Tyennan and Northeast Tasmania Elements have distinctly different magnetic signatures (Fig. 1b), the magnetic response of the dolerite sills within the Tasmania Basin obscures the location and nature of the boundary between these elements. Attempts to filter the magnetic signals to derive the basement signature give results that are interpretive at best (Gunn et al., 1997). The sills also degrade data from seismic reflection profiling, so the petroleum industry has not yet been attracted in large numbers to explore the Tasmania Basin. Therefore, deep seismic images of basement did not exist prior to the 1995 regional deep seismic program. In this paper we use the images from the deep seismic program to examine the architecture of the boundary between the Tyennan and Northeast Tasmania elements. In doing so, we infer a crustal extension event that previously had not been identified extensively in Tasmania.

2. The seismic program

Many of the crustal element boundaries can be traced offshore using regional magnetic and gravity data. Therefore, the bulk of the regional deep reflection profiling was conducted at sea close to the shoreline (Fig. 1) (Hill et al., 1995). Apart from being logistically easier than profiling in many places onshore, this had the advantage of being able to avoid many of the dolerite sills of the Tasmania Basin in the southeast. Nevertheless, several crustal elements could not be mapped offshore, and three short lines were recorded onshore (lines 1–3, Fig. 1). Two additional short onshore lines (lines 4 and 5, Fig. 1) were experiments designed to test parameters for recording within the dolerite sills of the Tasmania Basin (Barton et al., 1995).

The offshore seismic reflection program required the recording of 13 profiles (offshore lines 1, 4–15, Fig. 1), resulting in a circumnavigation of the island. Thirty-three portable seismographs were deployed across the island to record the energy from the ship's airguns in order to collect crustal scale refraction data (Chudyk et al., 1995). The University of Tasmania operates eight permanent seismic observatory stations, and their seismograms were captured digitally. Very little information on the crustal structure of Tasmania was available during the planning stages of the experiment. The crustal models of Richardson (1981, 1989) indicate that a maximum recorder spacing of 70 km would ensure that all seismic phases from all of the offshore seismic lines were recorded by at least part of the seismograph network.

3. Seismic refraction results

Data from the refraction and tomography

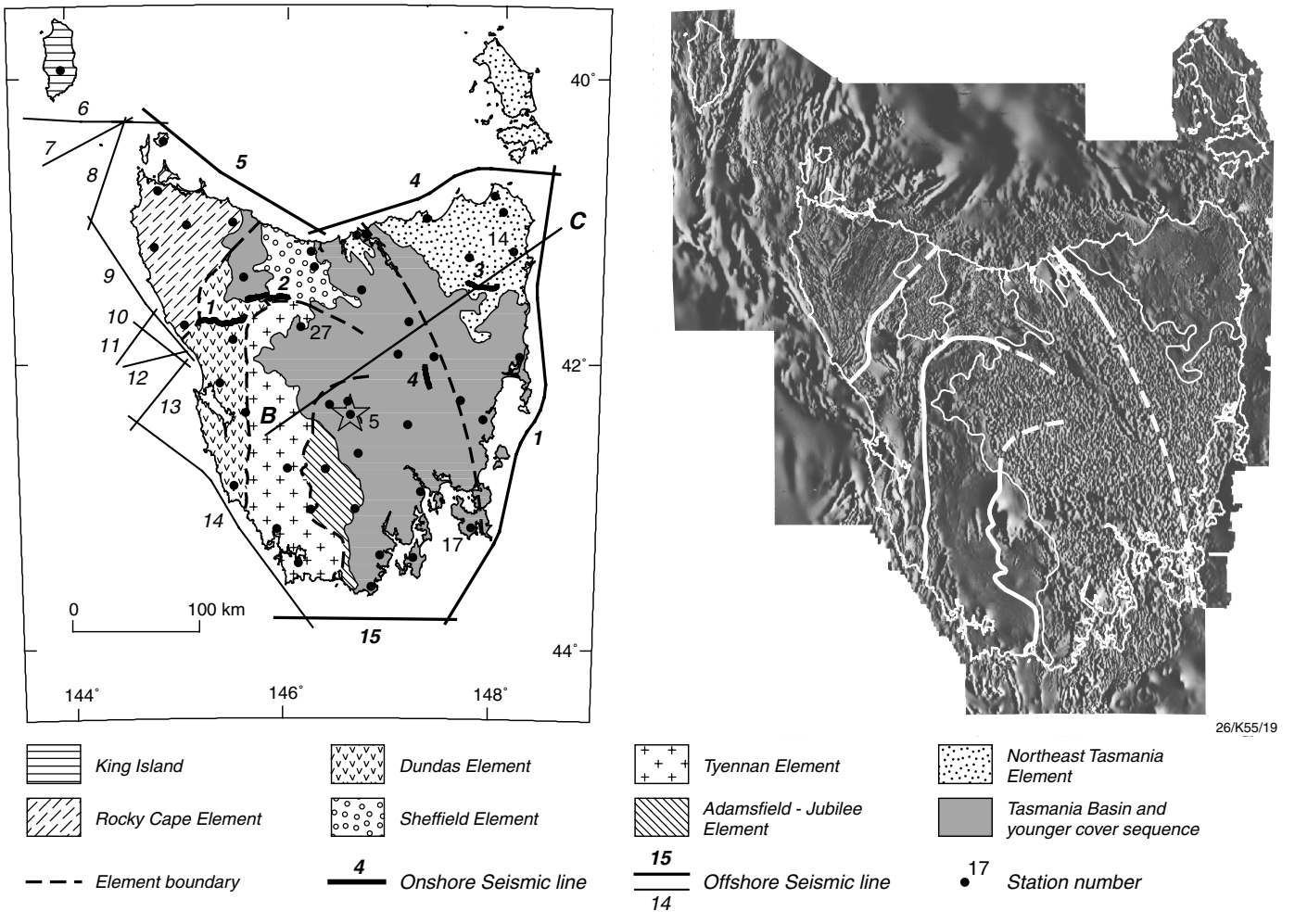

Fig. 1. (a) Major crustal elements of Tasmania. Position of seismic reflection profiles onshore and offshore are shown. The offshore profiles used in this study are in heavy lines. Refraction recording stations are shown as dots. Numbers show those referred to in Figs. 2 and 3. Star shows position of onshore blasts. BC shows the position of diagrammatic cross-section in Fig. 9. (b) Map of regional magnetic field, with element boundaries marked.

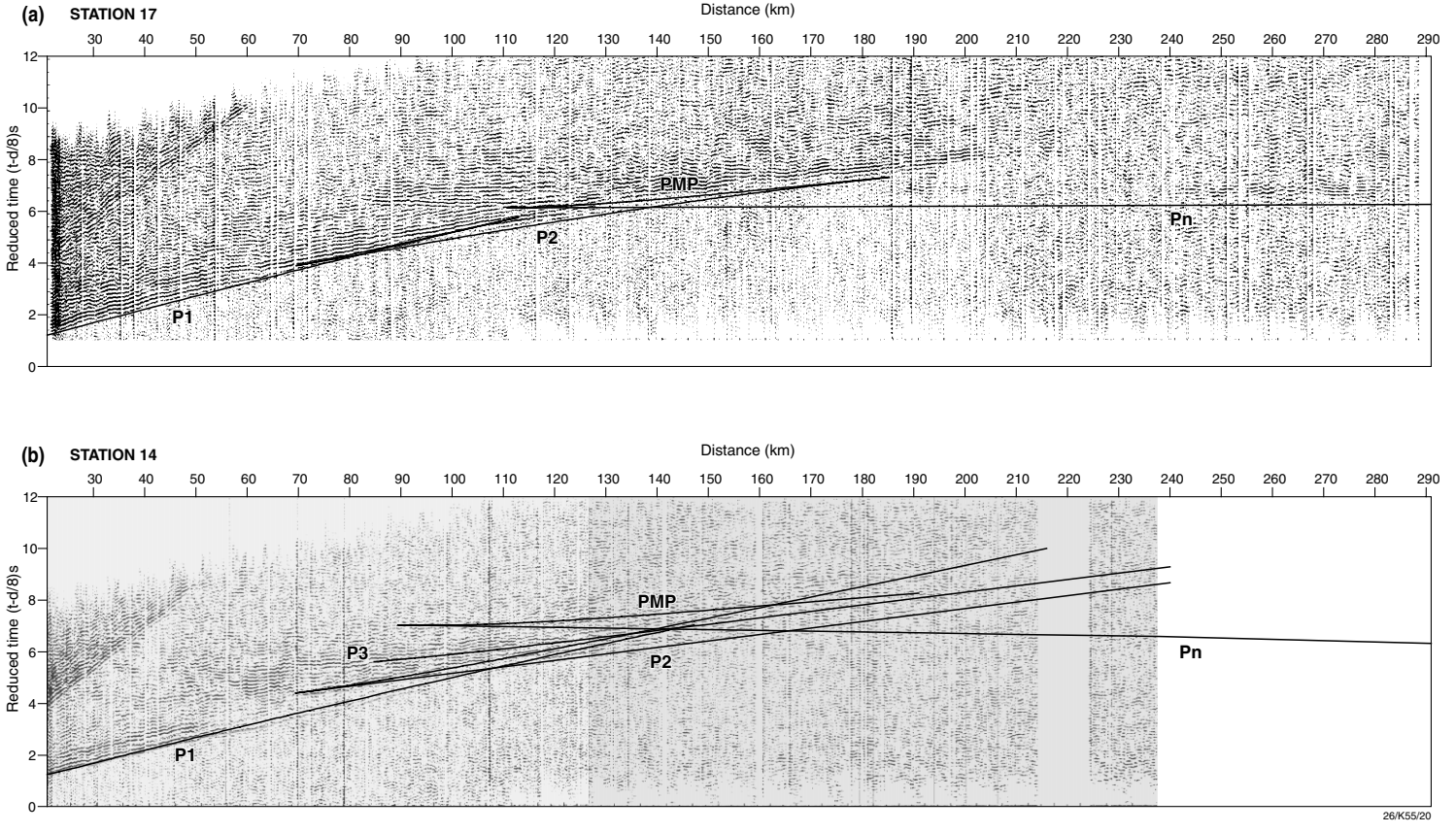

Fig. 2. (a) Seismic record section for refraction Station 17 near the SE coastline north along offshore Line 1. (b) Seismic record section from Station 14 in the NE south along offshore Line 1. For both sections, shot spacing was 50 m. Data are displayed in variable area format with a reduction velocity of 8.0 km s^{-1}. No coherency filtering was applied, and the amplitudes are trace-normalized. Travel time curves were calculated for the respective 1D crustal velocity–depth models in Fig. 3b.

Table 1
1D velocity–depth models for Stations 17 and 14 based on seismic data recorded from airgun blasts along offshore Line 1

Station 17		Station 14	
Velocity (km s^{-1})	Depth (km)	Velocity (km s^{-1})	Depth (km)
2.50	0.0	3.27	0.0
2.50	0.1	3.27	0.3
5.63	0.2	5.68	0.4
5.72	3.5	5.85	5.0
5.88	8.8	6.00	11.6
6.25	11.3	5.93	13.1
6.88	28.1	5.95	14.5
7.92	33.1	6.17	15.7
7.92	44.4	6.65	16.7
		6.65	19.2
		6.12	19.3
		6.06	23.7
		7.05	24.2
		7.00	26.3
		6.40	26.7
		6.40	32.6
		8.14	34.8
		8.25	47.0

component of the seismic program are currently being interpreted by both forward and inverse 1D, 2D and 3D modelling. The 1D models from forward modelling of two stations (14 and 17, Fig. 1) near the east coast are presented here, and used below to assist in the interpretation of the reflection data.

The data from Station 17 recorded from airgun blasts to the north along Line 1 are shown in Fig. 2a. The travel time curves superimposed on the record section are for post-critical reflection and refraction branches calculated for the model listed in Table 1 for Station 17. The model for Station 17 would be expected to represent the crust along the southern part of Line 1, and is shown in Fig. 3 as a velocity versus vertical two-way-travel time (TWT) curve superimposed on the reflection data from Line 1. The upper and lower crustal phases (P1 and P2, respectively) occur as first arrivals to 140 km. The mantle reflection PMP is strong as a later arrival between 80 km and its asymptote with P2 near 200 km; it is interpreted to be sub-critical at distances between 80 and 100 km. The upper mantle refracted phase (Pn) is weak beyond its cross-over to a first arrival near 160 km to about 230 km. Wide angle reflected phases can be interpreted linking refracted phases, so no low velocity layers are required by the data. A mid-crustal discontinuity is inferred, and the concave downwards curvature of the time–distance branches for the P1 and P2 phases requires positive velocity gradients in the upper and lower crust.

The data for Station 14, recorded from airgun blasts to the south along Line 1 (Fig. 2b) would sample the crust in the northern and central part of Line 1. The data from Station 14 have several significant differences from those of Station 17. Firstly, the phase P1 is strong at distances to about 50 km, but is weak beyond that. P2 occurs as a first arrival from about 105 km but is weak beyond its cross over with Pn at about 160 km. At large distances, it is parallel to, but offset by approximately a second, from a strong phase (P3) which is interpreted as evidence of third, deep crustal layer that was not identified in the data from Station 17. P3 is particularly clear at its retrograde cusp near 80–90 km. The slope of the P3 phase is such that it appears to cross PMP, rather than asymptote with it. The concave upwards nature of the P3 phase suggests that it is a reflection off a boundary, rather than a refracted wave that penetrates the boundary. The absence of clear refracted phases linking concave upwards (reflected) phases suggests that low velocity layers are present at depth. Finally, PMP is much weaker than in the data from Station 17.

The model for the data from Station 14 is listed in Table 1 and shown in Fig. 3 as velocity versus vertical two-way time. It has a distinctly different lower crustal character than that for Station 17. The lower crust is modelled as a series of alternating low and high velocity layers. This must be seen as a 1D representation of a 3D crust consisting of low velocity rocks mixed with high velocity rocks. The ambiguity in interpreting low velocity layers in seismic refraction data is such that a range of different velocity functions could be used within the low velocity layers. In this model, the velocities were constrained at the lower end to values that are reasonable for a middle to lower crust of felsic composition (e.g. Christensen and Mooney, 1995). At the higher end, the velocities in the low velocity layers were constrained by the interpreted position of the critical distance of reflections from the top of the underlying high velocity layer; this is very interpretative and not entirely robust.

Despite the ambiguity in the model for Station 14,

the data and the derived models from Stations 14 and 17 illustrate clearly that the crust in the northern part of Line 1 is different from that in the south.

4. Seismic reflection results

4.1. Offshore Line 1

The seismic reflection data from offshore Line 1 are shown in Fig. 3. The upper panel shows uninterpreted post stack migrated data. The data were migrated using a velocity function derived from laterally smoothing and reducing the stacking velocities (100% at the surface, 75% near the Moho). The migration velocities are very close to the independently derived velocities from the refraction data (Fig. 4). The migrated data contain very few migration 'smiles'.

The reflection data from Line 1 show a mostly non-reflective upper crust along the entire line, and distinctly different reflection characters in the middle to lower crust in the north and south, consistent with the evidence from the refraction data from Stations 14 and 17 that the crust in the north is different from that in the south. In the south, where the refraction model for Station 17 shows a positive velocity gradient with depth throughout the crust, the middle to lower crust is poorly reflective. In the north, where the refraction model shows alternating high and low velocity layers, the middle to lower crust is more strongly reflective. Fig. 3b summarises the interpretation for Line 1; Figs. 5–7 contain examples of the different types of crustal reflectivity along Line 1.

The Moho is interpreted along the entire Line 1 as a relatively strong continuous set of reflections near 11 s TWT in the south, shallowing to the north towards the middle of the line at a series of ramps, (each laterally about 10–20 km wide, e.g. near shotpoint 800, and between shotpoint 1200 and 1600). It correlates well with the transition in refraction velocities from less than 7.0 km s^{-1} in the lower crust to near 8.0 km s^{-1} below the Moho (Fig. 3b). The poorly reflective crust in the south is crossed by a number of gently south-dipping reflections that sole onto the Moho, usually near one of the ramps in the Moho. In Fig. 5, the Moho (M) is arrowed at just below 9.5 s TWT in the south and just above 9.5 s TWT in the north. One of the south-dipping reflectors is marked FB. The relative weakness of crustal reflections is demonstrated by noting that the reflectivity in the crust above and below the reflector FB is comparable to that of the mantle below the Moho, which is usually non-reflective. The south-dipping reflectors extend upwards into the upper crust, where together with north-dipping reflections, they define a geometry in the middle to lower crust suggestive of tilted fault blocks in extended crust (Fig. 3b). In Fig. 6, the reflection defining the top of one of the fault blocks (T) is seen to truncate against the side of another (FB). Seismic velocities range from 6.25 km s^{-1} below the mid-crustal boundary to less than 6.9 km s^{-1} in the lowermost crust, and are indicative of a felsic to intermediate lower crust probably containing rocks that are unlikely to have significant impedance contrasts, and hence are poorly reflective.

The fault block geometry of the lower crust changes to highly reflective lower crust north of about shotpoint 4000 (Fig. 3) (see also Barton, 1999). The change is accompanied by an increase in crustal thickness. In Fig. 7, the lower crustal reflections are mostly south-dipping. Individual reflections can seldom be followed for more than 10 km, and most fall into groups that are discordant with adjacent groups. We infer that the reflections come from highly folded rocks. However, some reflections fall into bands which are more continuous than other groups of reflections. They dip south and extend from the Moho to the top of the reflective lower crust (TS1 and TS2 in Fig. 7) and divide the lower crust into discrete packages. They are marked by thicker lines in Fig. 3b. The reflective lower crust reaches its maximum thickness between shotpoints 5000 and 6000. It correlates with the zone of alternating high and low velocity layers in the 1D velocity model from Station 14. The reflection Moho is less distinctive than further south and is defined as the base of the lower crustal reflectivity. It correlates with the refraction Moho from Station 14.

4.2. Offshore Line 15

Windows of Proterozoic basement in the Tasmania Basin imply that parts of the southern end of Line 1 are across Proterozoic basement. Line 1 joins Line 15 in the south (Fig. 1). Line 15 crosses the offshore

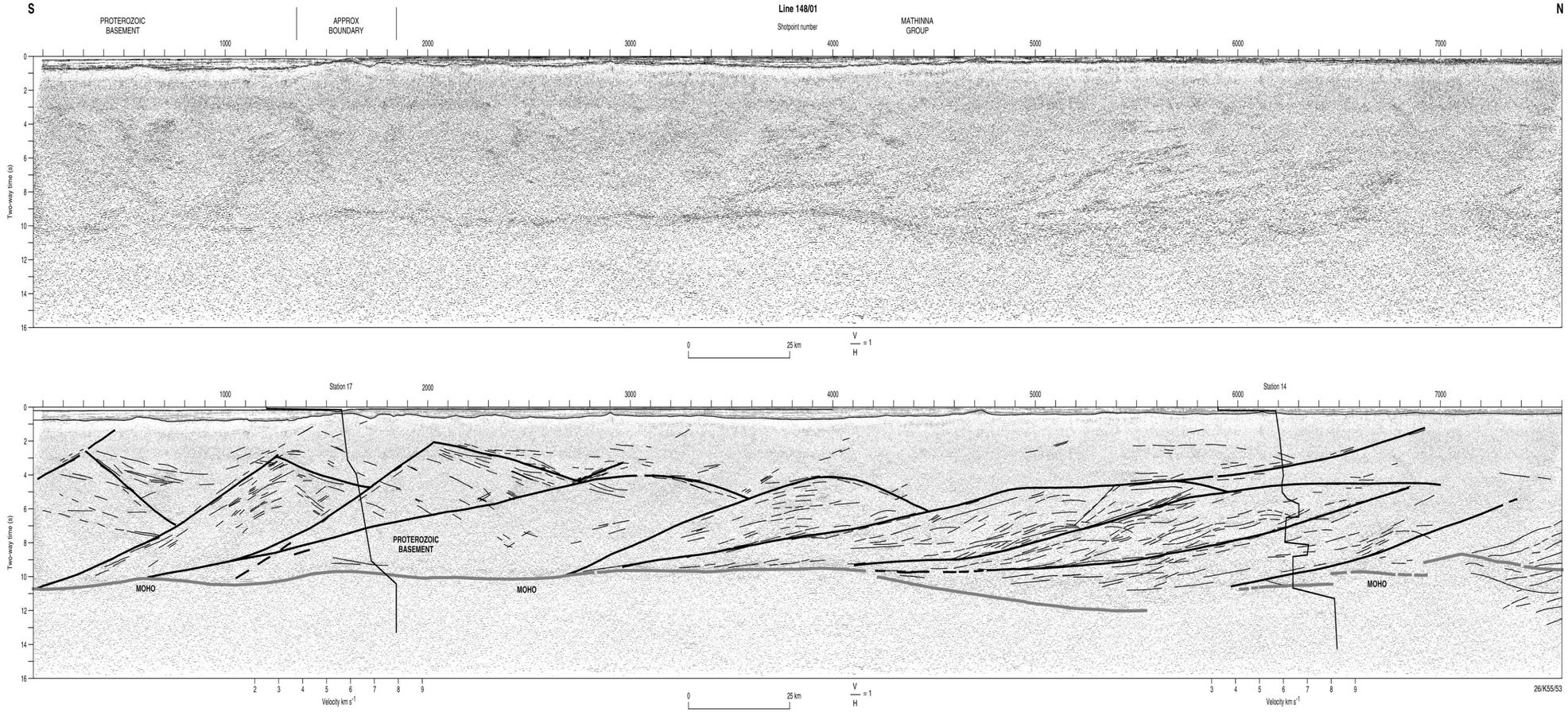

Fig. 3. (a) Seismic reflection data from offshore Line 1. Data are post stack wave equation migrated. $V/H \sim 1$ (assuming a seismic velocity of 6.0 km s^{-1}). (b) Interpreted reflection section. 1D models of velocity vs two-way-travel time were derived for the data in Fig. 2.

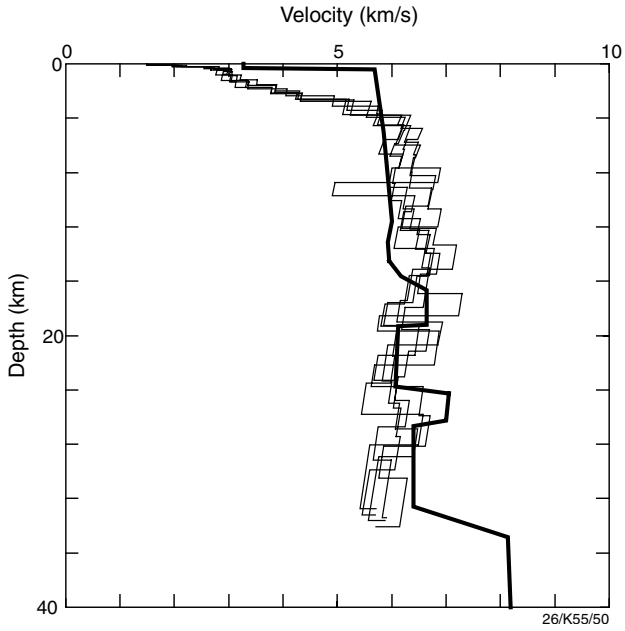

Fig. 4. Interval velocities used to migrate the seismic data from a 32 km section of offshore Line 1 near Station 14 (fine lines), and the 1D velocity–depth function from data recorded at Station 14 (bold line).

southern extension of the Proterozoic Tyennan Element, and therefore provides a link between the southern end of Line 1 and Proterozoic basement. The results for Line 15 are summarised in Fig. 8 as a line drawing of the reflections.

The western half of Line 15 across Proterozoic basement is largely non-reflective, except for weak reflections which mostly dip east. Onshore, the Tyennan Element consists mainly of polydeformed and metamorphosed Proterozoic quartz-rich clastic sedimentary rocks with minor metamorphosed igneous rocks and also minor younger sedimentary rocks (Seymour and Calver, 1995). Its regional magnetic signature is featureless (Fig. 1b), suggesting that these rocks continue to considerable depths. The non-reflective nature of the seismic data imply crust containing rocks with few impedance contrasts. In the west of Line 15, the reflection data cannot distinguish any difference between the upper and lower crust.

The eastern boundary of the Tyennan Element dips east from the surface beneath the Adamsfield–Jubilee Element. At shotpoint 2700, at a depth of about 18 km (6 s TWT), the boundary intersects a relatively strong and continuous reflection which dips west and soles out just above the Moho, which lies at about 11 s TWT. The sedimentary rocks of the Adamsfield–Jubilee Element are sub-horizontal to gently west-dipping against the Tyennan basement. Onshore, the Adamsfield–Jubilee Element consists of a deformed but unmetamorphosed succession of Neoproterozoic to Middle Palaeozoic sedimentary rocks of similar thickness to that observed in offshore Line 15 (Seymour and Calver, 1995).

5. Discussion

Although the refraction models for Stations 14 and 17 (Fig. 3b) are simple and 1D, they are consistent with the interpretation of the reflection data. The interpretation of the crust of the Tyennan Element along Line 15 can be traced into Line 1, where the lower crust is interpreted to be broken into a number of tilted fault blocks. The poorly reflective signature of Proterozoic crust can be followed north to about shotpoint 3500. The lower crust is much thicker than the non-reflective upper crust.

Further north, however, around shotpoint 4000, the fault blocks lie deeper in the crust and give way to the slices of reflective lower crust. Here, the boundary

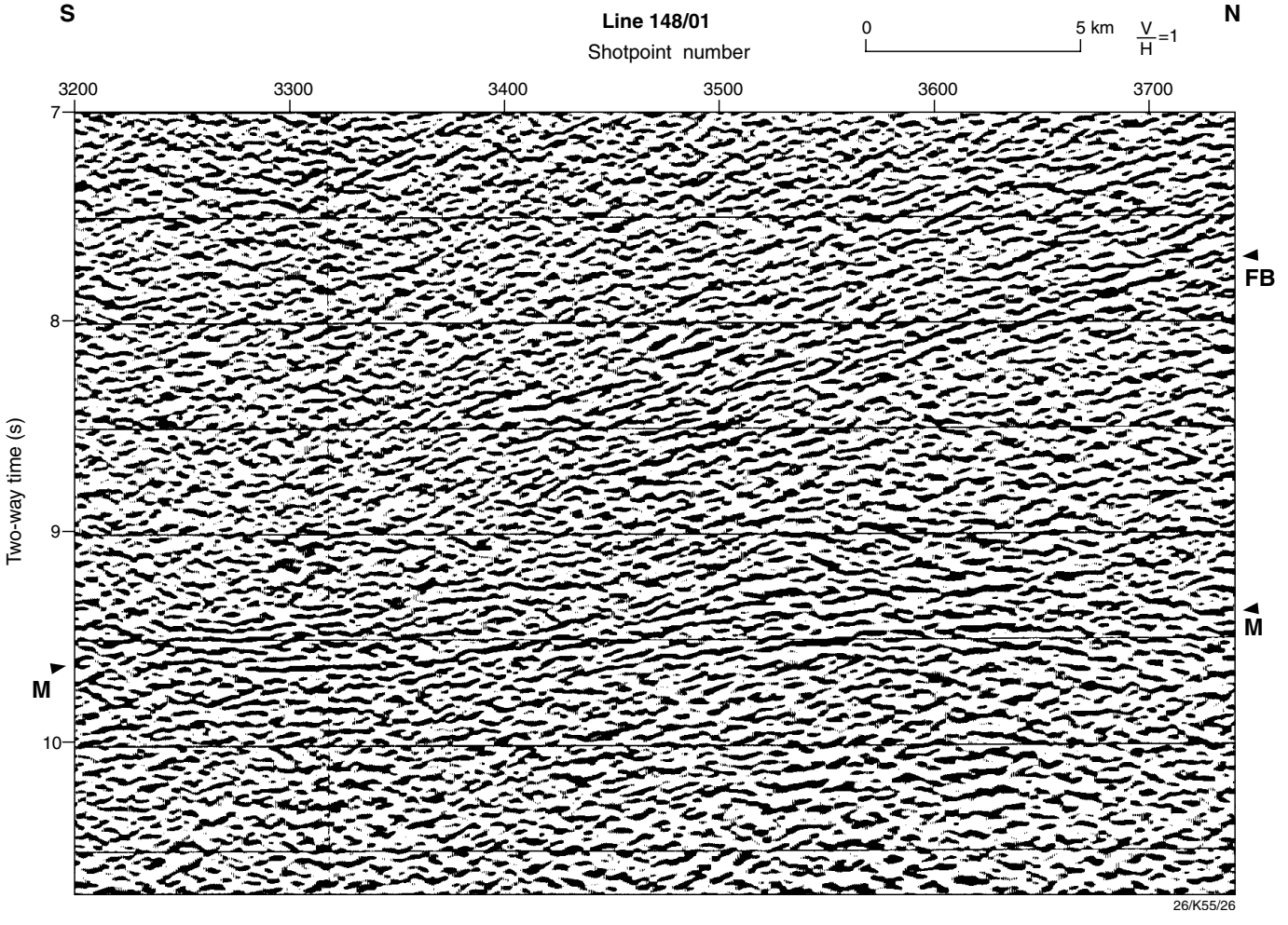

Fig. 5. Post stack migrated data from part of offshore Line 1 showing the lower crust and uppermost mantle under the extended Tyennan Element. M — Moho; FB — boundary between fault blocks. Refer to shotpoint numbers and time axis in Fig. 3 for section location on seismic line.

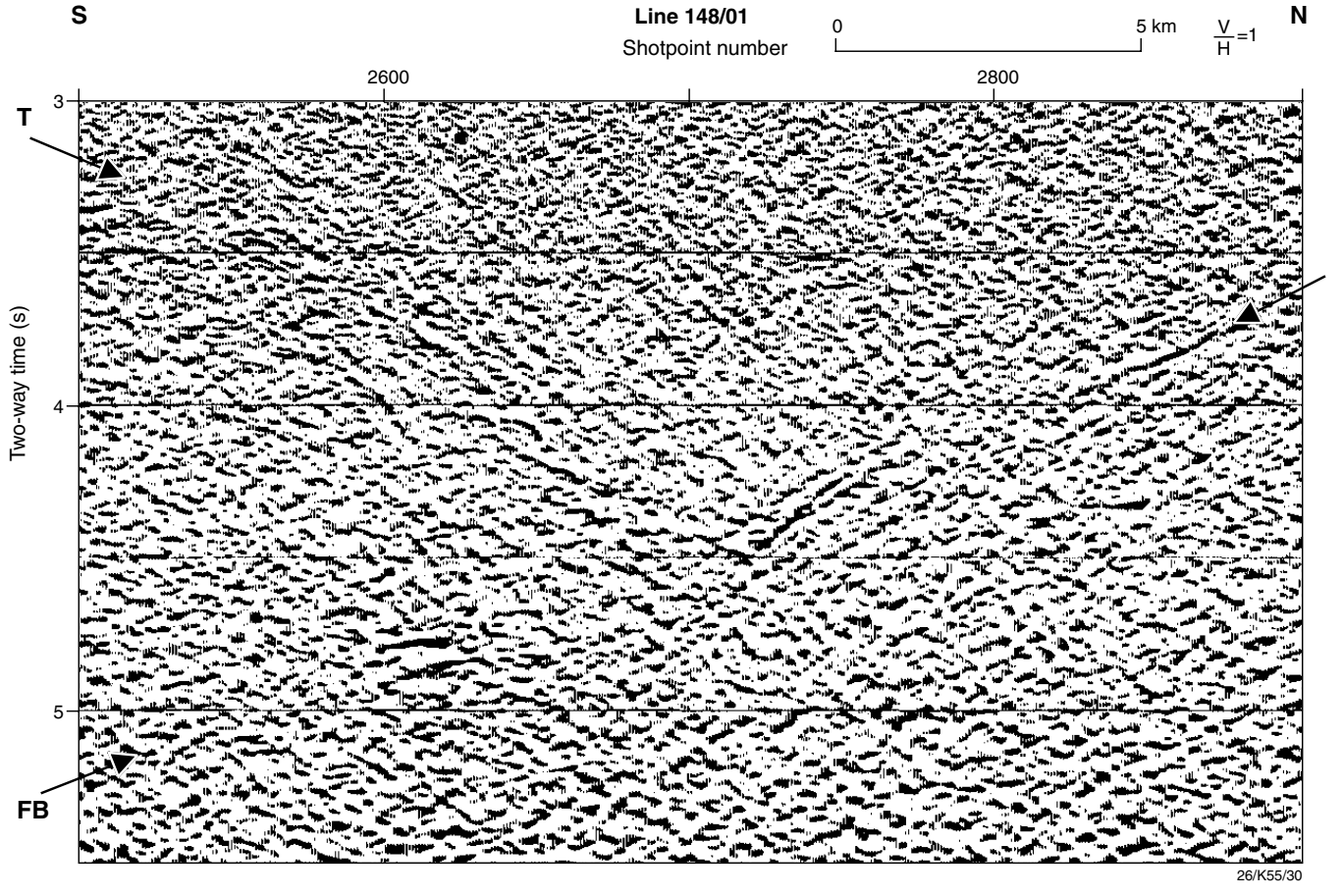

Fig. 6. Post stack migrated data from part of offshore Line 1 showing the top of one block fault (T) truncated against the side of another (FB). Refer to shotpoint numbers and time axis in Fig. 3 for section location on seismic line.

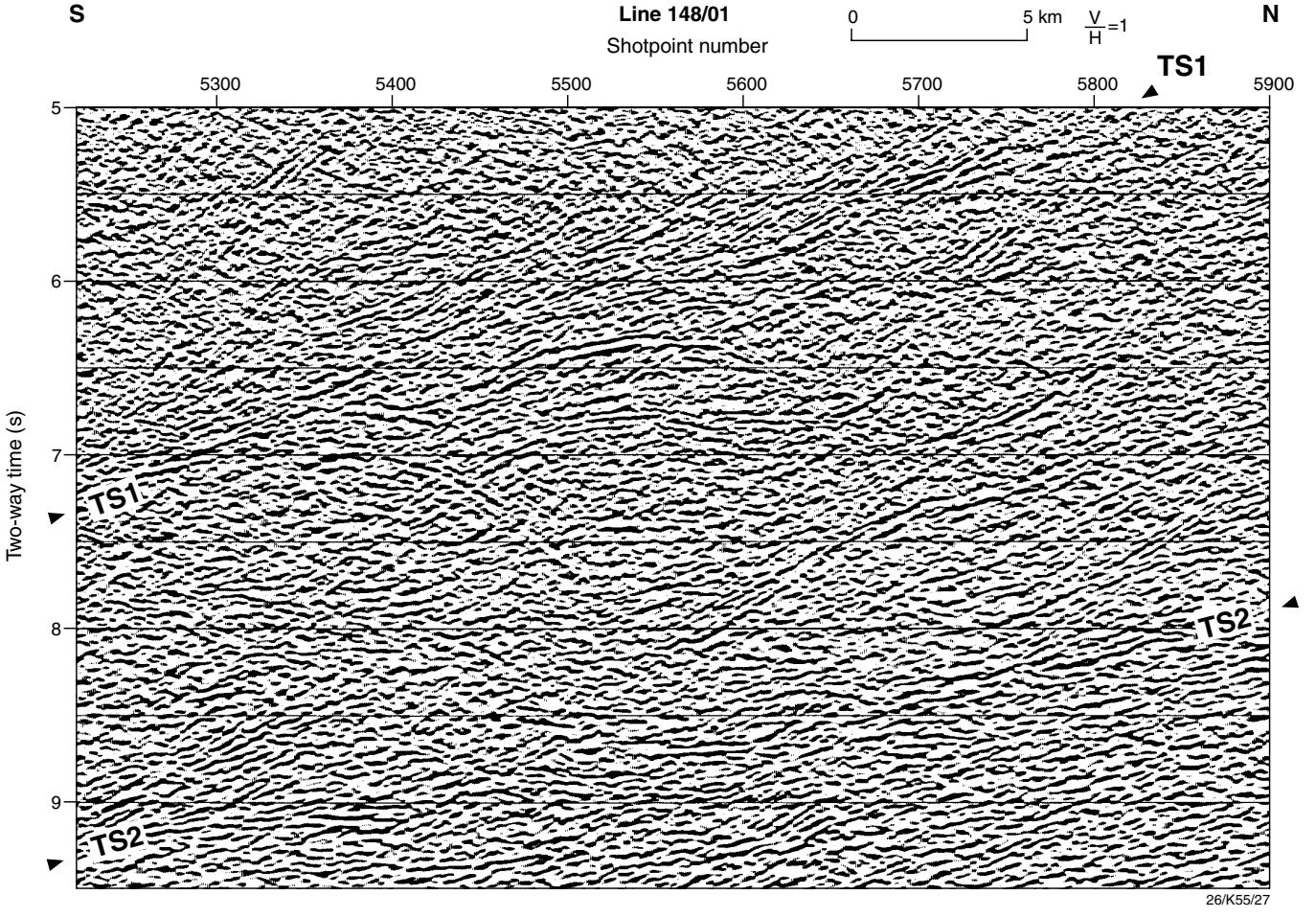

Fig. 7. Post stack migrated data from part of offshore Line 1 showing the reflective lower crust under the northern end of Line 1 under the Northeast Tasmania Element. Arrows marked TS1 and TS2 indicate interpreted boundaries between thrust slices. Refer to shotpoint numbers and time axis in Fig. 3 for section location on seismic line.

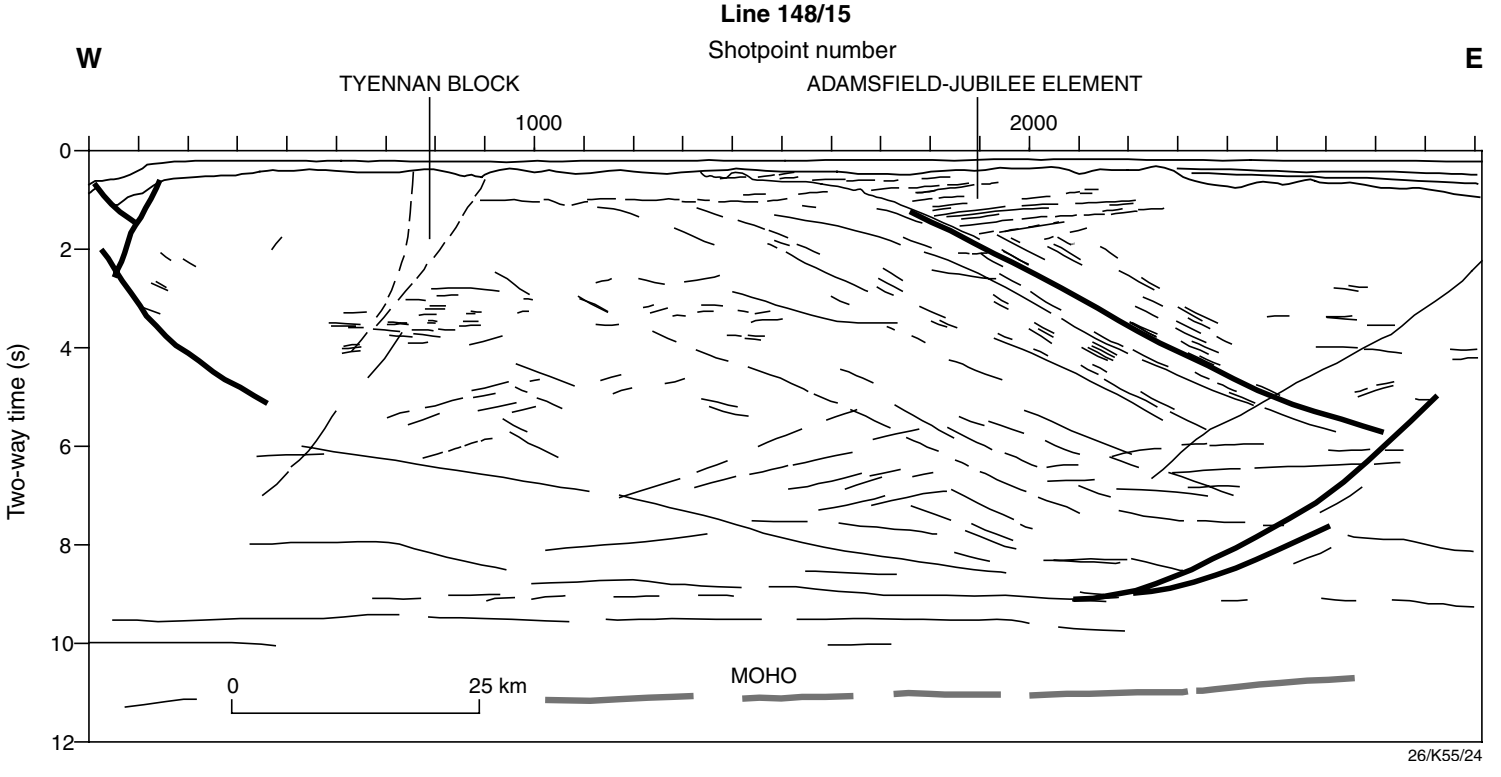

Fig. 8. Line diagram of offshore Line 15 along the southern coastline.

between the non-reflective upper and the reflective lower crust lies deeper, and the reflection Moho shallows. In the north of Line 1, the crust thickens and the boundary between the non-reflective upper crust and the reflective lower crust shallows.

The results from lines 15 and 1 are summarised in the diagrammatic cross-section in Fig. 9. The position of the cross-section is shown in Fig. 1a, and although the dips on boundaries in Fig. 9 are implied to be in the plane of the section, they are derived from apparent dips in lines 15 and 1, and may not be true dips. The tectonic interpretation implied in Fig. 9 and discussed below is based mostly on the geometry of the reflectors and the rock types that can be reasonably assigned on the basis of reflection strength and refraction-based velocities.

The Tyennan Element is interpreted as the basement block to an extended continental margin that formed to the east (1, Fig. 9). Its non-reflective character, and velocities less than 7 km s^{-1} are interpreted to imply mostly uniform, predominantly felsic composition rocks in the upper crust and felsic to intermediate rocks in the lower crust. The tilted lower crustal fault blocks (2, Fig. 9) are evidence for upper crustal extension that occurred by brittle failure. The reflections which define the boundaries of the fault blocks sole onto the Moho, indicating that the crust–mantle boundary in the south of Line 1 acted as a rheological boundary and probably a detachment surface during extension.

The age of the extension is debatable. Rocks of the Adamsfield–Jubilee Element onlap the Tyennan basement (3, Fig. 9), and are Neoproterozoic to Early Palaeozoic in age. We interpret equivalent rocks to occur above the rotated fault blocks to the east (4, Fig. 9). Two major extensional events are recognised in the Neoproterozoic of mainland Australia, one at ca. 830–725 Ma and the other at ca. 600 Ma (e.g. Lindsay et al., 1987; Lindsay and Korsch, 1991; Berry, 1995; Powell, 1996; Walter and Veevers, 1997). Events of these ages are expressed in Tasmania as the Cooee Dolerite (ca. 725 Ma) and lavas in the Smithton Basin in the northwest (Burrett and Martin, 1989). Powell (1996) favoured ca. 725 Ma as the timing of the breakup of the Rodinian supercontinent and the drifting away of Laurentia, but Walter and Veevers (1997) favoured the ca. 600 Ma event. The direction of extension was different for these two events, with the ca. 830–725 Ma extension being in a northeast–southwest direction (Powell, 1996) and the ca. 600 Ma extension being in a northwest–southeast direction (Lindsay and Korsch, 1991).

Using apparent dips on fault block boundaries from offshore seismic lines 15 and 1, the extensional faults dip towards the southwest, indicating that the extension direction was northeast–southwest. This suggests that the extensional event that stretched the eastern part of the Tyennan Element was probably related to the earlier Neoproterozoic (ca. 830–725 Ma) event, although the Late Neoproterozoic age (ca. 600 Ma) cannot be ruled out.

In contrast to the low reflectivity used to define the extensional tilted fault blocks, the strong reflections from the lower crustal rocks in the north on offshore Line 1 (5, Fig. 9) require large impedance contrasts. One explanation could be that the Jurassic dolerites comparable to those of the Tasmania Basin intruded a middle to lower crust of mostly felsic composition. However, we might expect dolerite sills to be mostly sub-horizontal, whereas the reflections observed in the data dip mostly to the south. An alternative interpretation can be based on interpretations of seismic and geological data from the possibly equivalent western Lachlan Orogen to the north in mainland Australia, where Gray et al. (1997) interpreted the strongly reflective crust to be caused by stacked oceanic crust. Such a model would explain the reflection strength here, particularly if the crustal shortening mixed possibly oceanic crust and sea floor sediments with fragments of highly extended continental crust. The data suggest that the shortening occurred by thrust stacking of slices defined by through-going reflectors (e.g. TS1 and TS2 in Fig. 7), with internal deformation within the thrust slices. Thickening of the original rocks by hundreds of percent is implied in the reflective lower crust.

Along offshore Line 1, the crust is thickest under the thickest section of reflective lower crust (5, Fig. 9). As the shortening is in the basement, presumably it predated the Early Palaeozoic deposition of the turbidites of the Mathinna Group of the Northeast Tasmania Element. In contrast, reflectors with a fan-like geometry at the tops of the extensional fault blocks (4, Fig. 9) could be syn-rift sedimentary rocks, and are largely undeformed; the upper reflections are sub-horizontal. Therefore, little or no

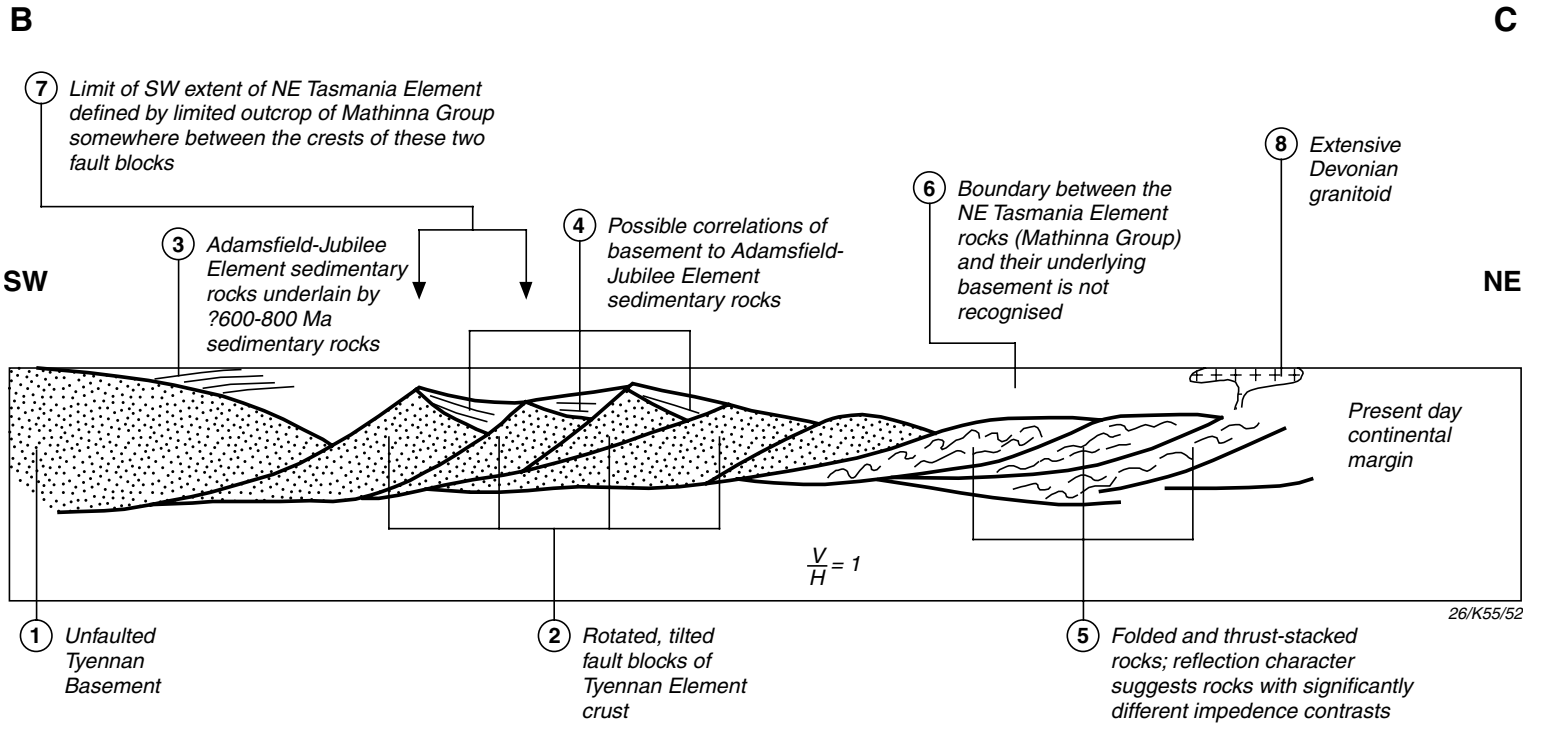

Fig. 9. Diagrammatic cross-section along the line BC in Fig. 1, based on the data from offshore lines 15 and 1.

shortening is inferred in the extended continental basement in the south. This suggests that the focus of deformation was in the northeast, and that the deformation did not propagate much into the region of extended continental crust.

The nature of the boundary between the sedimentary cover rocks of the Mathinna Group of the Northeast Tasmania Element and their underlying basement is not clear in the reflection data (6, Fig. 9) nor is the boundary that defines their southern extent under the Tasmania Basin cover rocks. From outcrop windows through the Tasmania Basin, it is known to occur in the zone marked 'APPROX BOUNDARY' in Fig. 3 (7, Fig. 9). This zone corresponds to the region between the crests of two tilted fault blocks, suggesting that one of them has provided structural control on the boundary. This would suggest that the Northeast Tasmania Element is a younger succession that formed outboard of an older, Neoproterozoic continental margin. It now lies above extended, block faulted crust, interpreted to be Proterozoic Tyennan Element in the south, and thinned continental margin and possibly oceanic crust of uncertain age in the north. This means that its surface position today cannot be used to infer the age of the underlying lower crust.

The tectonic model presented here is based on the crustal geometry interpreted in the reflection data, the relative amplitudes of reflections in the seismic sections, the velocities derived from the refraction data, and the need for consistency with the surface geology at the regional scale. Such a model is difficult to test by independent means. Also, based on the chemical composition of granites, Chappell et al. (1988) proposed that two basement terranes exist in Tasmania, a western Taswegia terrane and an eastern Bassian terrane. They inferred that the boundary was in a similar position to the element boundary on the southwest side of the Northeast Tasmania Element (Fig. 1). Fortunately, Devonian–Carboniferous granitic rocks were emplaced in all crustal elements after most of the tectonic processes discussed above had ceased (8, Fig. 9). One test of our tectonic model would be to use inherited zircon crystals from the granitic rocks to examine likely ages for the lower crust. Another test would be to see if further geochemistry of the granitic rocks can distinguish between different types of lower crust; for example, continental or oceanic, throughout the region. These tests have begun.

Acknowledgements

We thank Peter Hill, who was cruise leader for the offshore seismic profiling, Ed Chudyk and Ray Bracewell, who deployed the portable stations, and Joe Mifsud, who drafted the figures. The project was only possible because of the geological input from many staff at Mineral Resources Tasmania. In particular, we thank Claus Prodehl, Lincoln Hollister and an anonymous reviewer who provided comments that assisted in considerable improvements to the paper. B.J.D., R.J.K., A.N.Y. and T.J.B. publish with the permission of the Chief Executive Officer of the Australian Geological Survey Organisation. T.J.B. and N.R. publish with the permission of the Director of the Australian Geodynamics Cooperative Research Centre. A.V.B. publishes with the permission of the Tasmanian Director of Mines.

References

Barton, T.J., 1999. Crustal structure of northern Tasmania based upon a deep seismic transect. Geol. Soc. Aust., Abstr. 53, 3–4.

Barton, T.J., Johnstone, D.W., Richardson, R.G., 1995. TASGO seismic survey 1995: operational report. Australian Geological Survey Organisation, Record 1995/72.

Berry, R.F., 1995. Tectonics of western Tasmania: Late Precambrian–Devonian. Geol. Soc. Aust., Abstr. 39, 6–8.

Burrett, C.F., Martin, E.L., 1989. Geology and mineral resources of Tasmania. Geol. Soc. Aust. Spl. Publ. 15 (574pp.).

Chappell, B.W., White, A.J.R., Hine, R., 1988. Granite provinces and basement terranes in the Lachlan Fold Belt, southeastern Australia. Aust. J. Earth Sci. 35, 505–521.

Chudyk, E.C., Bracewell, R., Collins, C.D.N., 1995. Operational report for the 1995 seismic refraction, wide-angle reflection and tomography survey of Tasmania. Australian Geological Survey Organisation, Record 1995/74.

Christensen, N.I., Mooney, W.D., 1995. Seismic velocity structure and composition of the continental crust: a global view. J. Geophys. Res. 100, 9761–9788.

Drummond, B.J., Korsch, R.J., Barton, T.J., Brown, A.V., 1996. Crustal architecture in northwest Tasmania revealed by deep seismic reflection profiling. Australian Geological Survey Organisation, Research Newsletter, vol. 25, pp. 17–19.

Gray, D.R., Foster, D.A., Bucher, M., 1997. Recognition and definition of orogenic events in the Lachlan Fold Belt. Aust. J. Earth Sci. 44, 489–501.

Gunn, P.J., Mackey, T.E., Yeates, A.N., Richardson, R.G.,

Seymour, D.B., McClenaghan, M.P., Calver, C.R., Roach, M.J., 1997. The basement elements of Tasmania. Explor. Geophys. 28, 225–231.

Hill, P.J., Webber, K., Survey 148/159 Shipboard Party, 1995. Deep crustal seismic survey, circum-Tasmania and South Tasman Rise: AGSO survey 148/159 post-cruise report. Australian Geological Survey Organisation, Record 1995/27.

Lindsay, J.F., Korsch, R.J., Wilford, J., 1987. Timing the breakup of a Proterozoic supercontinent: evidence from Australian intracratonic basins. Geology 15, 1061–1064.

Lindsay, J.F., Korsch, R.J., 1991. The evolution of the Amadeus Basin, central Australia. Bur. Mineral Resour., Aust. Bull. 236, 7–32.

Powell, C.McA., 1996. Breakup and dispersal of the Rodinia supercontinent: implications for resource exploration. Geol. Soc. Aust., Abstr. 41, 351.

Richardson, R.G., 1981. Crustal seismology. PhD thesis, University of Tasmania, Hobart, unpublished.

Richardson, R.G., 1989. Crustal structure. Geology and Mineral Resources of Tasmania, Burrett, C.F., Martin, E.L. (Eds.), Geol. Soc. Aust. Spl. Publ. 15, 465–467.

Seymour, D.B., Calver, C.R., 1995. Explanatory notes for the time–space diagram and stratotectonic element map of Tasmania. Tasmania Geological Survey Record, 1995/1, 62 pp.

Walter, M.R., Veevers, J.J., 1997. Australian Neoproterozoic palaeogeography, tectonics, and supercontinental connections. AGSO J. Aust. Geol. Geophys. 17 (1), 73–92.